SELECTIVE DIRECTIONAL REINFORCEMENT OF STRUCTURES FOR MULTI-AXIS ADDITIVE MANUFACTURING

Sean Doherty[1], Wout De Backer[2], Arturs P. Bergs[3],
Ramy Harik[2], Michel van Tooren[2], Ioannis Rekleitis[1]
[1]Dept. of Comp. Science and Eng., University of South Carolina
301 Main Street
Columbia SC 29201
[2]McNAIR Research Center, University of South Carolina
1000 Catawba Street
Columbia SC 29201
[3]TIGHitco,
1375 Seaboard Industrial Blvd NW
Atlanta, GA 30318

ABSTRACT

Additive manufacturing has become a well-recognized method of manufacturing and has steadily become more accessible as it allows the designer to prototype ideas, products and structures unconceivable with subtractive manufacturing techniques for both consumer grade and industrial grade applications. In general, additively manufactured parts have reduced mechanical properties in the build direction of the print. Moreover, for shell-like structures, buckling is a dominant failure mode when loaded in compression, which introduces additional bending stresses in the interface between two subsequently printed layers. There is a need for reinforcement of both the material and the structures. A promising solution to the above mentioned problems is addition of local reinforcements constructed in the build direction of the base geometry. In this paper, a solution for these process defects and structural instabilities is proposed through modification of toolpathing and addition of both global and local features with multi-orientation slicing techniques. Designed for use with the broad range of capabilities of modern industrial robotics, a 6-axis directional reinforcement can be added to various types of base geometries. Through examples, two fundamental cases are elaborated: an example of the multi-axis deposition is discussed in this paper by adding a predefined feature to the side of existing geometry and in a second case, a set of global stiffeners is added to a base geometry. The methods discussed in this paper show great promise for additive manufacturing on 6 degree of freedom platforms.

1. INTRODUCTION

Additive Manufacturing (AM), in particular through the emersion and development of 3D printing, has been rapidly expanding throughout industry and hobby level manufacturing since its start in the 1980's. 3D printing and rapid prototyping techniques allow the designer to prototype ideas and devise products and structures unconceivable with subtractive manufacturing techniques. Since its recent booming, AM has become a well-recognized method of manufacturing and over the past decade, commercial and open source hardware and software have allowed the technology to steadily become more accessible and realistic for both consumer

grade and industrial grade projects, with its compound annual growth rate of 33.8 % over the last 3 years [1]. Reasons for this recent rapid expansion include the increase of the ability to produce increasingly more complex parts and the high demand for consumer level systems [2]. Multiple distinct approaches to additive manufacturing with distinct benefits in each method exist, and extensive summaries and comparisons have been performed by various authors [3],[4],[5],[6].

The toolpath planning proposed in this paper is designed with the method of Fused Deposition Modeling (FDM) in mind, a form of AM where thermoplastic material is heated above its glass transition temperature and extruded onto a base or itself through a nozzle, which is mobile with respect to the base. Due to the reduced complexity of the extrusion and curing process, this method of 3D printing has become the most widely used process to create end user products ranging from aerospace parts to consumer parts. Furthermore, modifying the extrusion process allows for composite additive manufacturing which further increases the capabilities. A part may be produced to include multiple types of polymers, filled polymers containing metal or fiber particles and polymer, and continuous fiber and polymer which is a process that can lead to strength increases up to 400 % with respect to the original unreinforced polymer [7], [8].

In this paper, the foundation of a solution for using multi-axis implementation based on the full range of 6 degree of freedom industrial robotics is proposed through modification of toolpathing and addition of features in the build direction of the base geometry. The solutions are to be implemented on a multi-axis additive manufacturing platform, where both relative translations and rotations of the deposition head with respect to the printed surface are possible in all directions, such as those shown in figure 1.

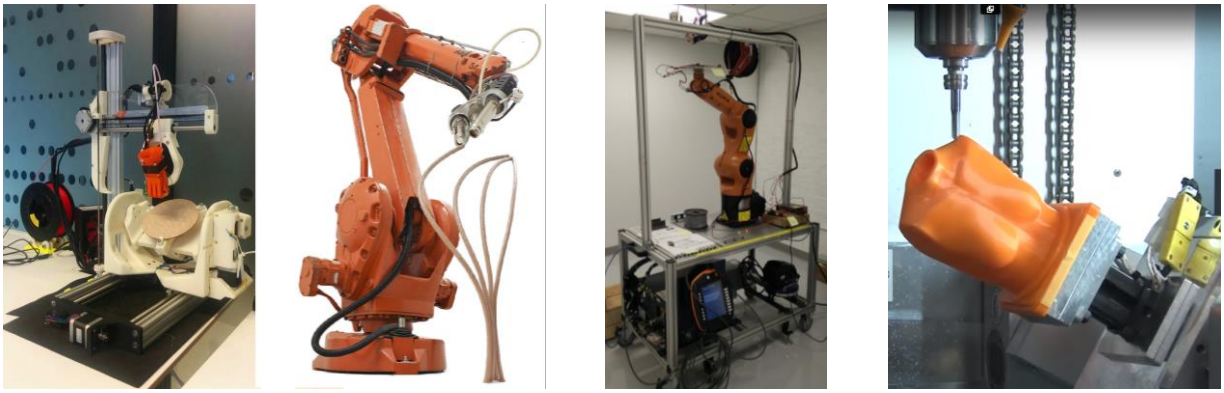

a b c d

Figure 1. State of the art 5 or 6 axis fused deposition modeling systems: (a) A 5 Degree of Freedom 3D Printer [9], (b) a nozzle end effector mounted to an industrial robot [10], (c) The in-house 6 degree of freedom printer in development at USC, (d) a 5-axis CNC milling machine outfitted additive-subtractive capabilities [11].

By using multi-orientation slicing and toolpath generation, reinforcement can be added to structures by adding either local features or global stiffeners, without the need of support material. Using the full range of capabilities of modern industrial robotics, a 6-axis directional reinforcement can be added to various types of base geometry. The addition of features to a base geometry is shown in two fundamental cases in this paper, discussing both printing orientation of

local features, and global stiffeners. For improved printing orientation of local features, an example of the multi-axis deposition is discussed in this paper by adding a predefined feature to the side of an existing geometry. For global stiffeners, a predefined slicing plane is used to identify a cross-section along which a stiffener is to be added. The methods discussed in this paper show great promise for additive manufacturing on 6 degree of freedom platforms.

2. STATE OF THE ART OF FDM

The growth and progression of additive manufacturing and 3D printing in particular has led to new issues concerning materials strength and reliability in geometries created with these new techniques. The mechanical properties of FDM produced parts are highly anisotropic in nature: the tensile strength of printed parts can decrease to as low as 10 % of their injection molded equivalent geometries purely depending on toolpath orientation and manufacturing method [12]. Additionally, experiments have shown that the modulus of elasticity can lower to 65 % [13]. In general, additively manufactured parts have reduced mechanical properties in the build, often the Z-direction, of the print. The toolpath orientation thus heavily influences the mechanical properties of the additively manufactured part. Therefore, the existing toolpath modules should be augmented with additive manufacturing toolpath generation algorithms to result in a desirable end result where full benefit can be made of the anisotropic mechanical properties [14].

Currently, the 3D printing of a predefined model begins with a geometric or volumetric representation of that part, usually in the form of a triangulated mesh in the form of an STL file or other similar representation. A set of desired toolpath parameters are also defined, providing quantification for process specific details such as part orientation and location, infill strategies, support material or outer shell thicknesses. Together with the set machine-specific parameters for the printer specifications (such as nozzle diameter, feed rate, etc.) and the material that is used (extrusion temperatures, viscosity…), the slicing software can generate layer-by-layer toolpaths. In order to be interpreted well by the hardware, usually some form of machine code is generated by the firmware in the printer, which translates the movement commands in stepper motor steps or movements. This process is visualized in figure 2.

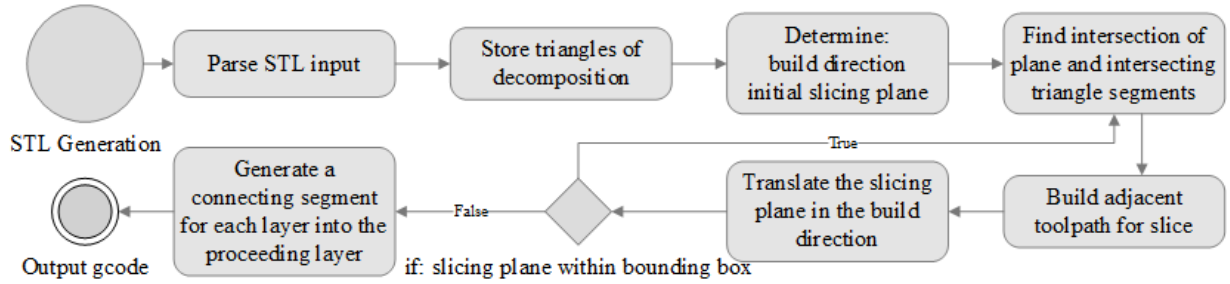

Figure 2. Conventional workflow operations in 3D printing.

2.1 Multi-Axis Toolpath Generation

Current, non-proprietary slicers focus on a parallel plane by plane approach to determine the toolpath, stemming from the limitation of current being able to print in the horizontal plane only. There has therefore not been a need to vary the orientation of the printing plane within the same print as there was not a mechanical system that could manufacture it. With the advent of 5 axis and 6 axis printers, toolpath generation can include varying plane orientation or base coordinate

system within the same model being printed [9], [10], [15], [16]. In addition, industrial robotics are becoming more widely used in the manufacturing world and many robots have full 6 degree of freedom capabilities [17]. Efficient toolpath generation and the reduction of support material is a critical challenge for FDM [18], and the further development of the software running these multi-axis systems can greatly reduce the need for support material. Further benefits include an increase in strength through higher continuity of filament and increased bonding of consecutive layers, as proven by methods for Curved Layer FDM (CLFDM) which allows deposition on a non-planar base surface as developed by , as shown in figure 3 [19]. This was implemented on a 3-axis system by [20].

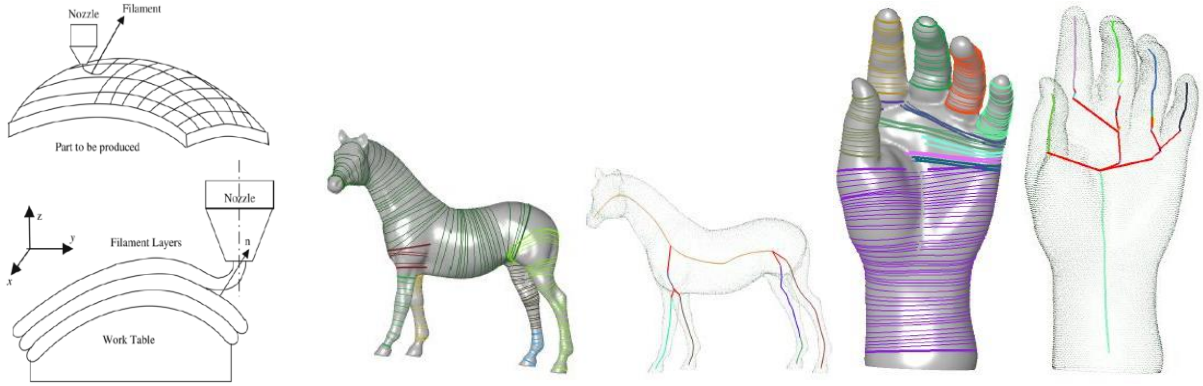

Figure 3. Novel methods in toolpathing and mesh analysis: (a) CLFDM methods may be applied to allow deposition on non-planar surfaces [19], (b) Toolpath and deposition orientation determination can be extracted from Prominent Cross-Sections (PCS) and skeleton analysis [21].

2.2 Build Orientation and Part Sectioning

The challenges to create a computer generated tool path for a Multi-Axis FDM system (MAFDM) include defining the slicing plane orientations, accurate sectioning of parts that benefits manufacturability, creating an efficient toolpath and maintaining product mechanical performance. Studies have shown that analysis on mesh-defined geometries can be used to identify and extract prominent cross-sections [21], excerpts of which are shown in figure 3. These studies can be used to aid in the sectioning and to determine general print build directions and nozzle orientations. Implementation in MAFDM requires significant improvements on the distinction for sections of transition. With this initial algorithmic analysis, further development could be implemented that allows for detailed user interaction for selecting the optimal build direction. In addition, an improved method of determining the build direction and depositing the material can benefit to further increase the mechanical properties and printer performance of the produced parts [22]. The continued investigation on the automated sectioning of a part to be printed for optimal build orientation is critical for future work.

3. COMPOUND FEATURE FUSED DEPOSITION MODELING

3.1 Elements of Geometry Slicing

To further the development of selective directional reinforcement of structures, a new elementary slicing tool was developed to generate toolpathing from Stereolithography file (STL) defined

geometries. Most commercially available CAD programs allow the exporting of the generated geometry into this format, which makes it a very suitable carrier format, though only geometry information can be carried, and material ID or other object-related properties cannot be stored. The STL format of a CAD part is the complete triangle decomposition of the geometry as extracted from the parametric surfaces defined in CAD through approximation values. Let T be the set of all triangles within the triangle decomposition and let triangle $t \in T$ be a triangle defined by three vertices v_1, v_2, $v_3 \in \mathbb{R}^3$. For a geometry where the Z-direction is the build direction, the top-level steps of the workflow functionality of a basic slicer is detailed:

1. Beginning at the minimum build direction (Z-direction) value over all vertices, a plane normal to the build direction is defined as the slicing plane (i.e. the XY-plane).
2. For every triangle $t \in T$ a test is performed to probe if exactly two of the vertices $v_i, v_j \in t$ lie on the opposite side of the slicing plane as the third vertex, v_k. If a triangle passes this evaluation, it is intersected by the slicing plane and the intersection line is found by interpolation of the line connecting vertices $v_i v_k$ and $v_j v_k$ on the slicing plane. These two intersecting lines are then added to the perimeter.
3. The slicing plane is offset in the positive build direction by the layer height and previous steps are repeated until no triangle intersects the slicing plane for the most extreme triangle in the build direction.
4. The layers are connected and infill strategies can be applied to fill the area between all perimeters.

Significant research efforts have been dedicated to minimizing manufacturing error in additive manufacturing, especially concerning errors stemming from the staircase effect or Z (height) error, as authors introduce correction methods such as adaptive slicing [23], [24]. For the slicing tool used in this paper, the algorithm terminates once the slicing plane has completed a slice that satisfies the condition: $V_{slicing\text{-}plane} \geq V_{max}$, where V_{max} is maximum distance of a vertex from the reference in the build direction $\boldsymbol{V}$ and $V_{slicing\text{-}plane}$ is the distance of the slicing plane.

3.2 Multi-Feature Compound Geometries

The above-described methodology of slicing and generating toolpaths for a geometry can be iterated upon, and as such, features (and toolpaths of features) can be added to reference or base features. For new features which have the same build direction of the base feature, the generation is as simple as extending the toolpath with the toolpath of the new feature. For compound geometries where features are added in random orientations, the situation is more complicated; as the slicer now needs a new build direction and a transition needs to be generated between the two or more features.

The idea of printing a geometry with features in different build directions is demonstrated with an example geometry with features in two orthogonal orientations, as shown in figure 3. Here, the portion of the geometry printed in the XY-plane is the **base feature** and the portion printed in the XZ-plane as the **extruded feature**. The defined build orientation of the base feature is the Z-direction, whereas the build direction of the extruded feature is the Y-direction. The manufacturing of this geometry will not result in a good quality print using the standard FDM process without support material with one build direction. The deposition angle thus has to be modified such that it is parallel and opposite to the build direction of the extruded feature. The

geometry shown in Figure 4 can be reproduced by separating the base and feature geometries on the STL level.

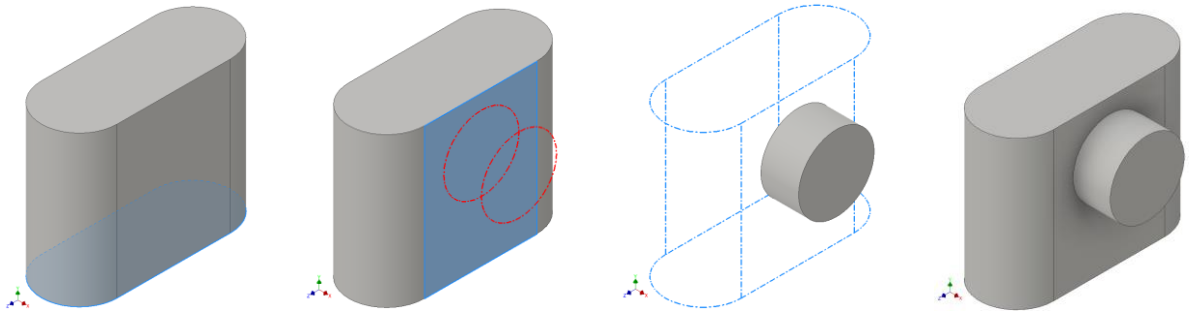

Figure 4. Example of building a compound geometry: (a) The base feature with build direction along the Z-axis, (b) the base feature with imposed trace of extrusion feature, (c) the extrusion feature with build direction along the Y-axis and (d) finally, the compound geometry.

Using this approach, a single toolpathing module can produce two distinct, disjoint toolpaths by offsetting the extrusion features build direction to match the new desired build direction. Once the two toolpaths have successfully been generated, a smart parent module can combine the full (base feature and extrusion feature) geometry by printing the base geometry as-is and then joining the subsequent toolpath end and starts such that no collisions occur between the tool and the geometry. The transition between the base feature and the extrusion feature is done here by:

1. Repeating the toolpaths of the final layer of the base feature with a safe offset in the build direction, until the toolpath reaches the point nearest to a point of the extrusion feature.
2. The deposition tool then orients along the extrusion base plane and traces the base feature to the start coordinate of the extrusion feature where the first command is tangent to the travel path.
3. After reaching the extrusion feature start point, the print will follow the conventional printing methods in the new feature-defined orientation.

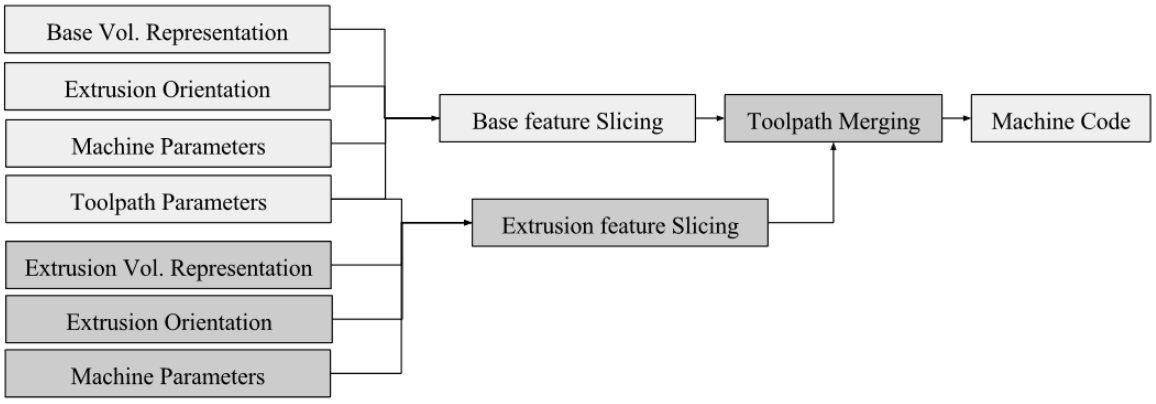

Figure 5. Conventional slicing (light colored) and new (dark colored) operations in 3D printing toolpath generation flow.

The new steps added to the conventional process from figure 2 are shown in figure 5. For processes that allow start-stop, such as FDM, the extrusion can simply be halted when tracing the extra layer on the base feature. For processes where start-stop is not present, the end product can undergo post-processing such as grinding to remove the excess deposition. The start point of the extrusion feature is an element of the closest slicing plane to the base feature surface; the connection segment is tangent to the curvature surrounding the start point. These constraints are in place to minimize the chance of collision and enforce a smooth transition from the end of the base feature to the beginning of the extruded feature.

3.3 Stiffener Generation

In addition to multi-feature compound 3D printing elaborated above, a second concept of multi-orientation printing can be captured in the form of stiffeners. Stiffeners are elements present in many structures where buckling due to compression or shear loading of thin-walled structures needs to be prevented, as is often the case for aerostructures. The base geometry's toolpath is constructed in the same way as the traditional method in the introduction, as was the case with the base feature of the multi-feature compound geometry toolpath generation. At this point, the two methodologies diverge. While in generating the extruded feature in the previous section we have a predefined geometry that already has the core of its toolpath defined, in this feature generation, a cutting plane is generated at a location where a stiffener is desired in the geometry. The intersection of this cutting plane, further defined as the **stiffener plane**, with the base geometry forms the foundation of the stiffener, and depending on the stiffener parameters, orbits and offsets are added to form multiple paths around the base feature. The method for generating the stiffener plane is as follows:

1. Three points, p_1, p_2, $p_3 \in \mathbb{R}^3$ within the bounds of the geometry are set to identify the orientation of a stiffener plane.
2. The stiffener plane is defined through vectors $\overrightarrow{v_1}$ and $\overrightarrow{v_2}$, where $\overrightarrow{v_1} = p_1 - p_2$ and $\overrightarrow{v_2} = p_1 - p_3$. The cross-product of these two vectors $\vec{n} = \overrightarrow{v_1} \times \overrightarrow{v_2}$, returns the normal (build direction) of the stiffener plane.

Once the stiffener plane has been defined, the procedure for the stiffener toolpath generation is as follows:

3. For each point q, of the base geometry's toolpath: $\vec{f} = q - q_i$ is defined, where q_i is any point within the stiffener plane.
4. The distance α from point q to the stiffener plane is then defined as:

$$\alpha = \frac{(\overrightarrow{f} \cdot \vec{n})}{|\vec{n}|} \quad [1]$$

5. A distance threshold, ε is used to select points from the base geometry to be considered for projection onto the stiffener plane: If $\alpha < \varepsilon$ then the point q is projected onto the stiffener plane to generate a projected point q_p via the following:

$$q_p = \begin{bmatrix} p_x - (\alpha A) \\ p_y - (\alpha B) \\ p_z - (\alpha C) \end{bmatrix} \quad [2]$$

where A, B, and C are the coefficients of the stiffener plane equation. The purpose of this $\alpha < \varepsilon$ constraint is to minimize projection error which smoothens the stiffener toolpath.

6. These steps are repeated to generate each stiffener ring.

Once the intersection of the base object with the stiffener plane has been computed for all stiffeners, the beginning of each toolpath or the first **orbit** (the notion here is that the stiffener rings will be a spiraling outward toolpath so each layer is referred to as an orbit) must be constructed by selecting a single point from the trace and determining the adjacent point to generate the toolpath. This is accomplished using a nearest-neighbor approach using the Euclidean distance as the metric. The result of this is a single ring tracing the cross-section of the base geometry at the given rings stiffener plane. During this calculation, the algorithm determines the centroid of the cross-section as the set of projected points is being iterated over. The user defines the desired amount of orbits, N, for the stiffener rings. Once all initial orbits have been constructed along with their centroid, the algorithm begins to generate the final toolpath via the following procedure:

7. For each orbit level, O ∈ [1, N] the parity of O is determined and, based on this, a decision is made whether to begin at the last stiffener ring or the first. This is done to minimize 1) the number of connection segments connecting each stiffener and 2) the initial connection between the end of the toolpath of the base geometry and the first stiffener ring to be printed.
8. If O is odd, then the iteration is begun by printing the orbit of the last stiffener ring. This enforces that the first orbit (i.e. O = 1) will begin on the last stiffener ring which is inherently the one closest to the end of the toolpath for the base geometry. Note that the algorithm begins with orbit ID O = 1 as the zeroth orbit's path is a collision with the shell of the base geometry at every point). If O is even, the orbit will begin from the first stiffener ring. For either even or odd, the orbits will be appended to the toolpath in order first → last or last → first, respectively.
9. At each stiffener plane, the following algorithm is proposed to successfully generate a collision free orbit:
10. For every point p ∈ Orbit(i), offsets d_X, d_Y, d_Z are determined by the following:

$$\begin{aligned} d_x &= [p_x - centroid(i).x] * c * O \\ d_z &= [p_y - centroid(i).y] * c * O \\ d_z &= [p_z - centroid(i).z] * c * O \end{aligned} \quad [3]$$

11. where Orbit(i) is the set of adjacent points from the i^{th} stiffener ring, centroid(i) retrieves the centroid for the i^{th} stiffener ring, O is the index of the orbit and c is the deposited road thickness, by which the orbits are offset each consecutive pass. The next point in the orbit's toolpath is then determined as:

$$p' = \begin{bmatrix} p_x + d_x \\ p_y + d_y \\ p_z + d_z \end{bmatrix} \quad [4]$$

12. Point p' is appended to the toolpath.
13. Once completing an orbit, the algorithm moves to the next or previous stiffener ring depending on the parity of O.
14. This process is repeated until the number of Orbits O = N.

The orientation of the tool is then determined from the projected local normal of the base geometry surface on the stiffener. The stiffener generation is qualitatively shown in figure 6. Following this iterative approach has shown to produce promising, collision-free toolpaths encompassing multi-orientation toolpaths. The complete part toolpath generation is then augmented as shown in figure 7.

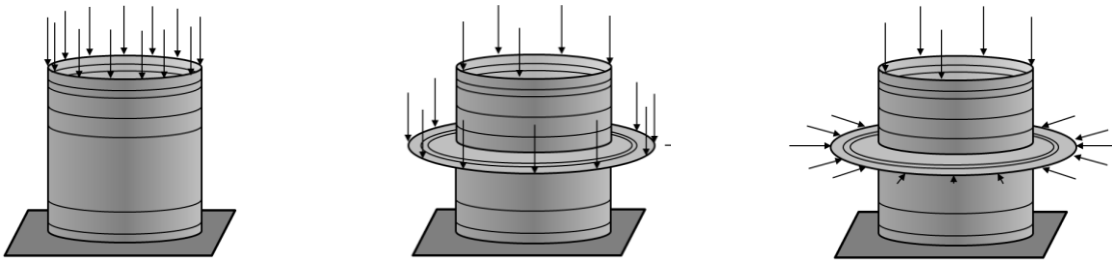

a b c

Figure 6. Stiffener generation: (a) the base geometry with (b) uncorrected and (c) normal-corrected tool orientation.

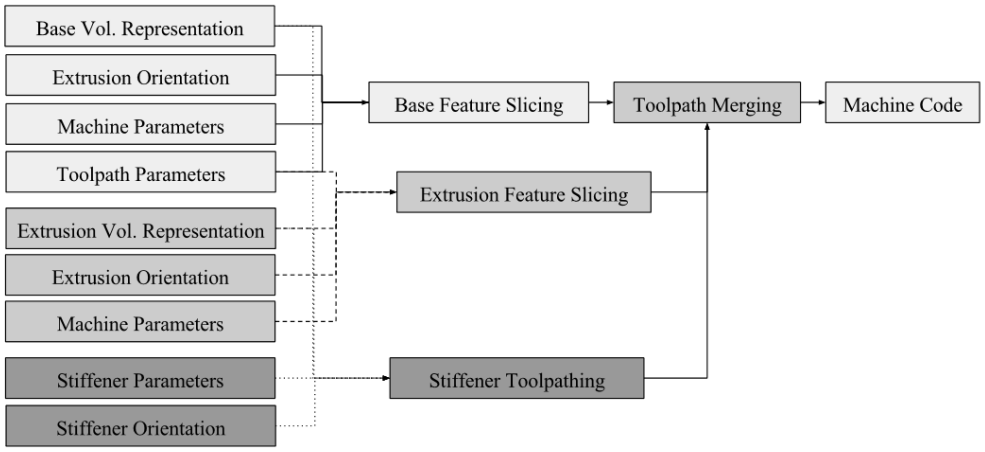

Figure 7. The complete workflow of extrusion and stiffener toolpath generation on top of a base geometry.

4. PRELIMINARY TOOLPATHING APPLICATIONS

Through the use of sample cases and geometries based on the application of the above methodology, several proof of concepts of varying complexity showing the exploration of the new toolpath planning of multi-orientation 3D printing are presented. The evaluation of the

proposed algorithms and resulting toolpaths is currently only based on ensuring the path is collision free, and that the results obtained are manually inspected to result in a feasible toolpath for manufacturing on a 6 degree of freedom system. In the near future, the physical systems capable of printing these parts will be used for physical application and evaluation of the proposed methods. Note that only the outer perimeter is shown for the toolpaths, as the infill shape or density is not relevant for the multi-orientation deposition proof of concept, and any infill is simply an addition to a layer's toolpath code.

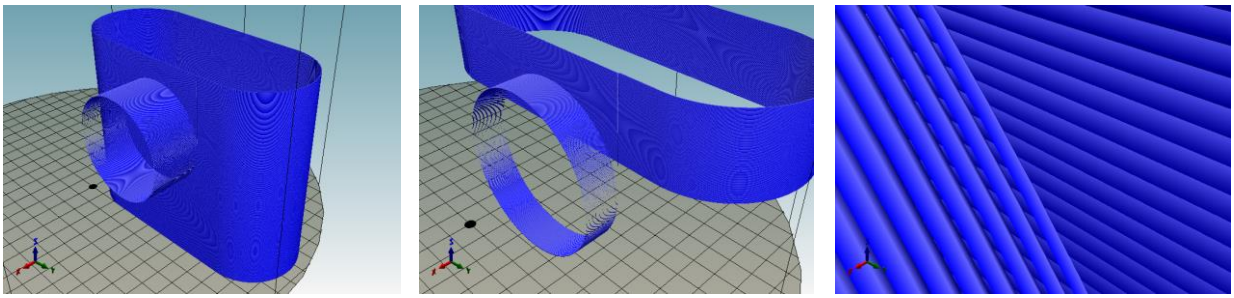

a b c

Figure 8. Compound geometry generated with the toolpath generator: (a) the full multi-planar deposition toolpath, (b) a section of the toolpath containing the transition, (c) and a close-up of the out-of-plane support showing the different orientation of the toolpaths.

The multi-base compound geometry module was used to create a multi-orientation object based on the example shown in figure 4; the results of which are shown in figure 8. The generated toolpath show promising results and no intersections were identified, proving that this is a feasible toolpath for such geometry. The toolpath can also be generated for non-orthogonal features, an example of which is shown in Figure 9. The only current limitation of the toolpath generator is that the support surface is required to be planar, and as such CLFDM can be implemented to further expand the capabilities of the code. Note that, due to limitations of the visualization engine, vertical extrusions are not visualized well.

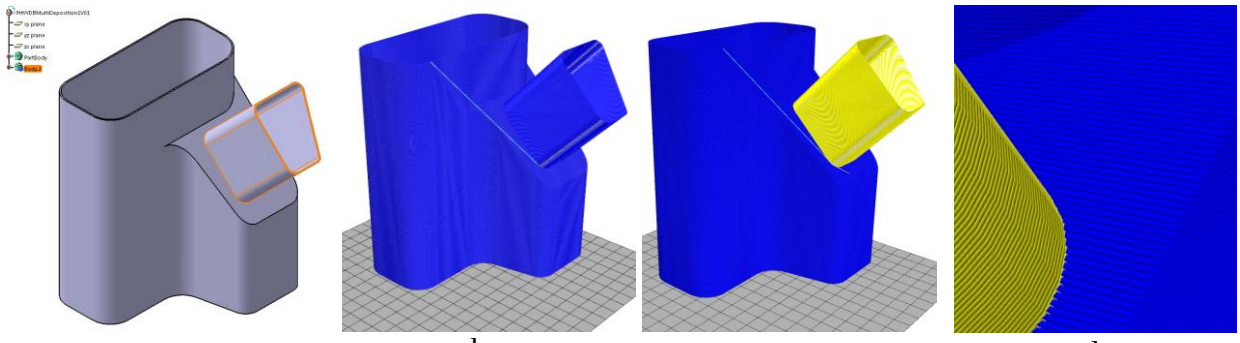

a b c d

Figure 9. Compound geometry generated with the toolpath generator: (a) the design model from Catia, (b) the full multi-planar deposition toolpath, (c) the extruded feature and (d) a close-up showing the different orientation of the toolpaths.

Similarly, the stiffener generation algorithm was applied to a simple cylinder. A set of parallel horizontal stiffeners were added at locations on the base geometry normal to the surface and build direction. The results of which are shown in figure 10. This algorithm has also been applied to more complicated base features of varying geometries as shown in figure 11.

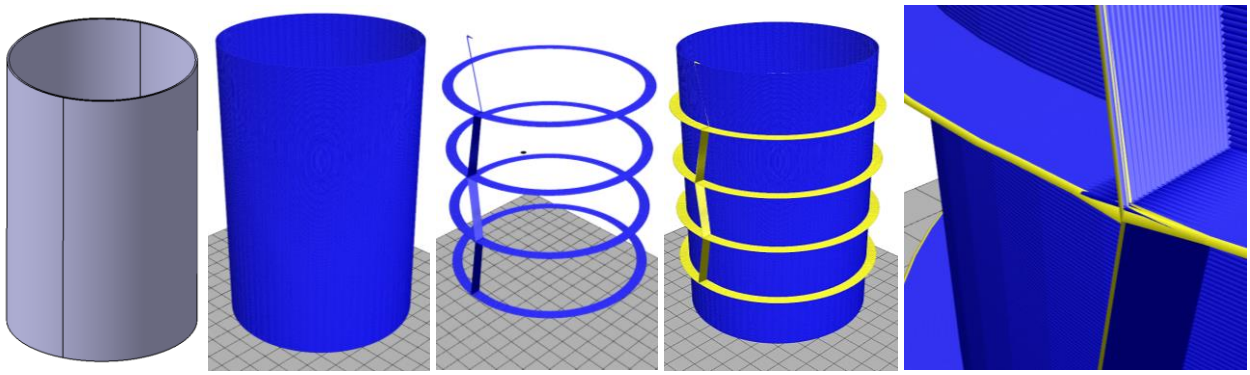

Figure 10. Stiffened cylinder generated with the toolpath generator: (a) the CAD-Defined geometry, (b) the base geometry, (c) the stiffener toolpath, (d) the highlighted stiffened geometry and (e) a close-up of the stiffener showing the different toolpath orientations.

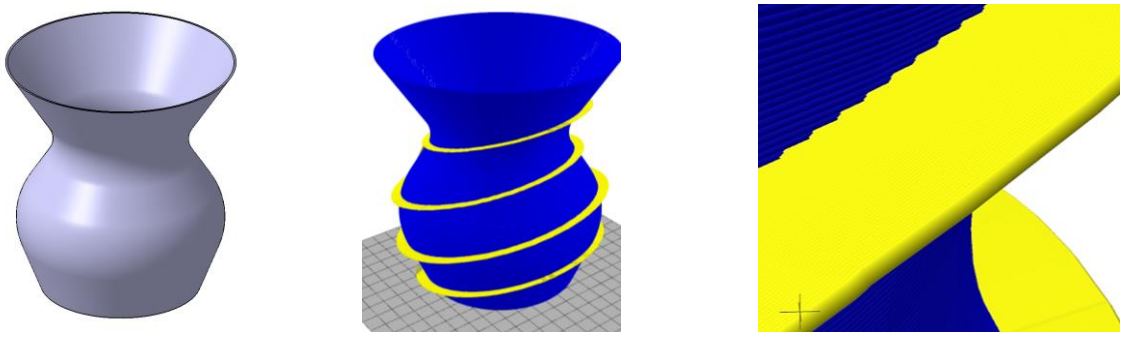

Figure 11. A randomly stiffened vase generated with the toolpath generator: (a) The CAD model, (b) the stiffened geometry, and (c) a close-up of a stiffener.

Finally, an example showing the combination of the two capabilities is shown in figure 12. Here, the base geometry is augmented with an extrusion geometry, which is then stiffened through a set of randomly oriented parallel stiffeners.

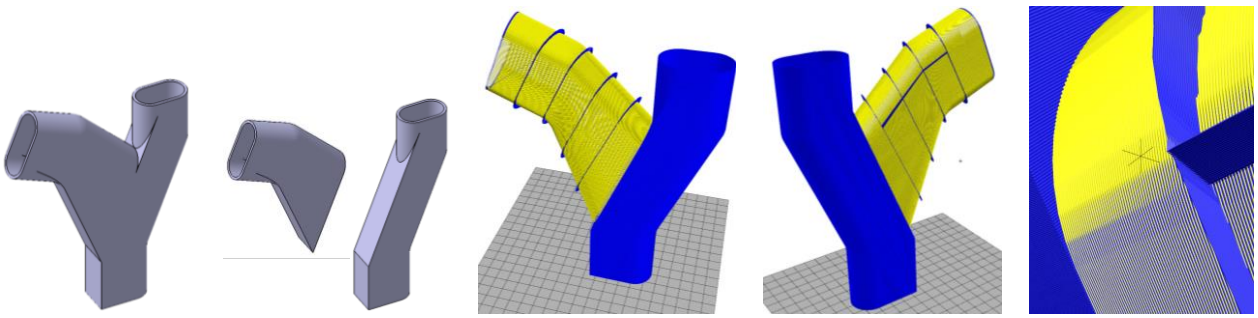

Figure 12. Stiffened, compound geometry generated with the toolpath generator: (a) the CAD Model of the compound object, (b) the base features, (c) & (d) the compound toolpath, (e) A close-up of the stiffened section showing the different toolpath orientations.

5. CONCLUSIONS

In this paper, studies concerning the state of the art and the necessity for multi-orientation toolpathing in additive manufacturing processes are reviewed in light of the emersion of 5 and 6-degree of freedom additive manufacturing hardware. The need for the ability to print in multiple orientations on a base geometry is a void in the current knowledge on toolpathing and with the interesting capabilities of 3d printing; it needs to be addressed to exploit the full benefit of this emerging technology. Two distinct methods were proposed to increase the mechanical behavior of Fused Deposition Modeled parts through the use of multi-axis hardware. The first one is to identify prominent cross sections and to define a build orientation based on this existing analysis method. Extrusion features can then be easily added to base features, taking into account that the transition between the two features does not cause a collision. The second method uses a base geometry and constructs orbits round the outer geometry generating stiffeners which can help the stability of thin-walled structures. Through the use of sample geometries shown the application of the above methodologies, proofs of concept to explore the toolpath planning of multi-orientation 3D printing are presented. The promising results presented in this paper allow for optimism that Multi-Axis Additive Manufacturing has a place in the future of manufacturing. However, significant efforts will continue to be required for these capabilities to be widely accepted and before 6-axis additive manufacturing processes become a standard in the manufacturing industry.

6. REFERENCES

1. Wohlers, .T, Caffrey, T., Campbell, I. “The Wohlers Report 2016”, *Wohlers Associates*, 2015, ISBN 978-0-9913332-2-6.
2. Gibson, I., Rosen, D. W., Stucker, B. “Additive Manufacturing Technologies”, *Springer*, 2010, ISBN 978-1-4419112-0-9, doi: 10.1007/978-1-4419-1120-9.
3. Yan, X. and Gu, P. “A review of rapid prototyping technologies and systems”, *Computer-Aided Design*, vol. 28, pp. 307–318, 1996.
4. Pham, D. T. and Gault, R. S. “A comparison of rapid prototyping technologies”, International *Journal of Machine Tools & Manufacture*, pp. 1257–1287, 1998.

5. Kruth, J. P., Leu, M. C., and Nakagawa, T. “Progress in additive manufacturing and rapid prototyping”, *Annuals of CIRP*, vol. 47(2), pp. 525–540, 1998.
6. Conner, B. P., Manogharan, G. P., Marthof, A. N., Rodomsky, L. M., Rodomsky, C. M., Jordan, D. C., and Limperos, J. W. “Making sense of 3d printing: Creating a map of additive manufacturing products and services”, *Additive Manufacturing*, vol. 1-4, pp. 64–76, 2014.
7. Mori, K.-I., Maeno, T., Nakagawa, Y. “Dieless forming of carbon fibre reinforced plastic parts using 3D printer”, *Procedia Engineering*, vol. 81, pp. 1595–1600, 2014, doi:10.1016/j.proeng.2014.10.196.
8. Matsuzaki, R., Ueda, M., Namiki, M., Jeong, T.-K., Asahara, H., Horiguchi, K., Nakamura, T., Todoroki, A., Hirano, Y. “Three-Dimensional printing of continuous-fiber composites by in-nozzle impregnation”, *Nature, Scientific Reports*, vol. 6, No. 23058, doi: 10.1038/srep23058
9. Grutle, Ø. K. “*Designing a 5-axis 3d printer*”, master thesis, University of Oslo, 2015.
10. Jokic, S. and Novikov, P. “Mataerial: A radically new 3d printing method”, 5 Feb. 2016. <http://www.mataerial.com/ >
11. Stevenson, K. “Can ENOMOTO’s Experimental 5-Axis 3D Printer Hybrid Do The Impossible?”, May 2, 2016, <http://www.fabbaloo.com/blog/2016/5/2/ can-enomotos-experimental-5-axis-3d-printer-hybrid-do-the-impossible>
12. Ahn, S. H., Montero, M., Odell, D., Roundy, S., and Wright, P. K. “Anisotropic material properties of fused deposition modeling abs”, *Rapid Prototyping Journal*, vol. 8, pp. 248–257, 2002.
13. Ziemian, S., Okwara, M., and Ziemian, C. W. “Tensile and Fatigue behavior of Layered ABS”, *Rapid Prototyping Journal*, vol. 21 (3), pp. 270–278, 2002, DOI 10.1108/RPJ-09-2013-0086.
14. De Backer, W., Harik, R., van Tooren, M. J., Tarbutton, J. A., and Gürdal, Z. “A framework for automated additive-subtractive manufacturing of multi-material composites”, *Proceedings of TMCE 2016*, May 9–13, Aix-en-Provence, France, pp. 317-328, 2016
15. Molitch-Hou, M. “A new spin on 3d printing weaves objects without supports”, 24 May 2016. <http://www.engineering.com/3DPrinting/3DPrintingArticles/ArticleID/11939 /A-New-Spin-on-3D-Printing-Weaves-Objects-without-Supports.aspx>
16. Zhang, Y., De Backer, W., Harik, R., and Bernard, A. “Build Orientation Determination for Multi-material Deposition Additive Manufacturing with Continuous Fibers”, *Proceedings from the 26th CIRP Design Conference*, pp. 1–6, 2016
17. West, D. M. “The impact of emerging technologies on employment and public policy”, *Brookings Center for Technology Innovation*, pp. 1–22, October, 2015
18. Ding, D., Pan, Z., Cuiuri, D., Li, H., Larkin, N., van Duin, S. “Automatic multi-direction slicing algorithms for wire-based additive manufacturing”, *Robotics and Computer-Integrated Manufacturing*, vol. 37, pp. 139–150, 2016, doi:10.1016/jrcim.2015.09.002.

19. Chakraborty, D., Reddy, B. A., Choudhury, A. R. “Extruder Path Generation for curved layer Fused Deposition Modeling”, *Computer-Aided Design*, vol 40, pp. 235–243, 2008, doi:10.1016/j.cad.2007.10.014.

20. Singamneni, S., Roychoudhury, A., Diegel, O., Huang, B. “Modeling and evaluation of curved layer fused deposition”, *Journal of Materials Processing Technology*, vol. 212, pp. 27–35, 2012, doi:10.1016/j.jmatprotec.2011.08.001.

21. Sellamani, S., Muthuganapath, R., Kalyanaraman, Y., Murugappan, S., Ramani, K., Hoffman, C. “PCS: Prominent Cross-Sections for Mesh Models”, *Computer-Aided Design & Applications (CAD&A)*, vol. 7, No. 4, pp. 601–620, 2010

22. Zhang, Y., Bernard, A., Harik, R., Karunakaran, K. P. “Build orientation optimization for multi-part production in additive manufacturing”. *Journal of Intelligent Manufacturing*, pp. 1–15, 2015, doi: 10.1007/s10845-015-1057-1

23. Kulkarni, P., Dutta, D. “An accurate slicing procedure for layered manufacturing”, *Computer-Aided Design*, vol. 28, No. 9, pp. 683-697, 1996.

24. Koc, B., Lee, Y.-S. “Adaptive Ruled Layers Approximation of STL Models and Multiaxis Machining Applications for Rapid Prototyping”, *Journal of Manufacturing Systems*, vol. 21, No. 3, 2002.